Multi-polarized Spectrum Sensing in Correlated and Uncorrelated Channels[☆]

Ali Panahandeh[a,b,*], Claude Oestges[b], Jean-Michel Dricot[a], François Horlin[a], Philippe De Doncker[a]

[a] *OPERA Department, Université Libre de Bruxelles (ULB), CP165/81 avenue F.D. Roosevelt 50 1050 Brussels Belgium*

[b] *ICTEAM Electrical Engineering, Université catholique de Louvain (UCL) place du Levant 3, 1348 Louvain-la-Neuve, Belgium*

Abstract

Compared to classical spatially separated multiple antenna system, cross-polarized co-located antenna systems are an interesting way to reduce equipment size while reducing the inter-antenna correlation. In this paper the spectrum sensing of a Cognitive Radio (CR) system taking advantage of polarization diversity under Rayleigh fading is investigated and compared to an equivalent system using spatial diversity. This analysis is based on a theoretical formulation applied to a real-world scenario. For this purpose, an outdoor-to-indoor measurement campaign at a frequency of 3.5 GHz is realized, where an indoor secondary user senses the signals received from an outdoor primary base station. The signals received in each antenna are first combined and then applied to an energy detector. The theoretical expressions are simulated in the measurement context. The detection probability behavior as a function of distance between the Primary Transmitter (PTx) and the Secondary Terminal (STE) and the inter-antenna correlation effect on the sensing performance are studied.

Keywords: Cognitive Radio, Polarization, Sensing, Energy detector, MIMO

1. Introduction

In recent years, the demand for radio-frequency spectrum is increasing as the interest of consumers in high data rate wireless services is growing. However, with most of the spectrum being already allocated by governmental regulators, it is becoming extremely hard to find vacant bands to deploy new services [1]. On the other hand, based on FCC report [2], many portions of the allocated frequency bands are not used for significant periods of time.

Cognitive Radios (CR) are proposed as an interesting way to more efficiently use the frequency resources [3, 4]. A CR network is deployed on the same frequency band allocated to an existing primary network without interfering with it. A CR Secondary User (SU) finds the frequency bands which are not utilized by Primary Users (PU) and communicate on them. In order to satisfy the primordial non-interfering condition, the SU must be able to detect reliably and quickly the presence of a PU in a frequency band [5]. Different spectrum sensing techniques have been proposed so far in the literature [1, 6]. Among them, Energy Detection (ED) has been widely applied since it does not require any a priori information about the primary signal and has much lower complexity [7, 8].

However in practice, spectrum sensing is con-

[☆]This work is supported by the Belgian National Fund for Scientific Research (FNRS-FRS) - FRIA

[*]Corresponding author - Phone number: +3226503087, Fax number: +3226504713

Email addresses: Ali.Panahandeh@ulb.ac.be (Ali Panahandeh), claude.oestges@uclouvain.be (Claude Oestges), jdricot@ulb.ac.be (Jean-Michel Dricot), fhorlin@ulb.ac.be (François Horlin), pdedonck@ulb.ac.be (Philippe De Doncker)

siderably deteriorated by the fading nature of wireless channels so that a PU could be completely hidden from a SU. Multi-antenna sensing has been proposed as an interesting way to reduce channel fading effects by introducing spatial diversity into the spectrum sensing scheme. Several previous works have already treated the application of energy detector on a multiple antenna system [9–15]. It has been found that the poor sensing performances of a single antenna system are considerably improved by the use of spatial diversity at the Secondary Terminal (STE). However, there are two limiting issues in the use of spatial diversity which could be resolved by the use of co-located cross-polarized MIMO antennas at the STE.

First of all it is shown in [11] that in correlated channels the sensing performance of a multi-antenna CR system using spatial diversity is degraded; hence, to benefit from diversity, a large inter-antenna spacing is required to lower the inter-antenna correlation, which tends to increase the terminal size. The use of three perpendicularly polarized co-located antennas on the other hand, would let the STE be almost as compact as a single antenna system while enjoying the benefits of diversity by the low inter-antenna correlation which exists between cross-polarized antennas [16–18].

Secondly, the polarization of the transmitted primary wave is randomized owing to the different interactions with the surrounding environment so that the signal received at the STE is composed of many waves with different polarizations. This polarization variability is not exploited in the spatial diversity case, and depending on the primary transmitted polarization and the orientation of the STE, the sensing performance could be deteriorated. This issue could be solved by the use of three perpendicularly polarized antennas which receive all incident polarizations.

In the absence of major results in this field, this paper investigates the sensing performance of a CR system using a tri-polarized antenna at the STE and in a real-world scenario. This analysis is based on an outdoor-to-indoor measurement campaign, where the secondary network is deployed indoor and senses the signals received from an outdoor primary base-station.

Based on the results obtained from this measurement campaign and a theoretical formulation described later in this paper, the sensing performance of an energy detector applied to a three-polarized antenna where each antenna experiences different uncorrelated Rayleigh fading is studied and compared to the spatial diversity case where the STE is made of three co-polar separated antennas. The detection probability behavior as a function of distance between PTx and STE and the inter-antenna correlation effect on the sensing performance are studied.

The paper is organized as follow: In section II the problem of primary signal detection in a tri-polarized reception scenario is formulated. Section III presents analytical formulations in a deterministic channel scenario. Section IV treats the case of Rayleigh fading channel. The measurement campaign is presented in section V. Section VI presents the results obtained from the simulation of the theoretical expressions in the measurements context. Section VII concludes this paper.

2. Problem formulation

We consider a CR receiver made of M antennas (with $M = 3$ for the particular case of three cross-polarized antennas). Considering a signal bandwidth W and an observation time T over which signal samples are collected (chosen so that the time-bandwidth product TW be an integer), the goal is to determine whether a signal is present (hypothesis H_1) or not (hypothesis H_0).

Under H_1, the primary transmitted signal $s(t)$ is received at the i^{th} CR receiver antenna over channel h_i and additive zero mean white Gaussian noise $n_i(t)$. The signal $s(t)$ is assumed to be unknown deterministic signal. The received signal $r_i(t)$ at the i^{th} receive antenna is then obtained under the two hypotheses by:

$$\begin{cases} H_1 \ : \ r_i(t) \ = \ h_i s(t) + n_i(t) \\ H_0 \ : \ r_i(t) \ = \ n_i(t) \end{cases} \tag{1}$$

In the unrealistic scenario where the received signals on each antenna are uncorrelated, by com-

bining the signals received on each antenna by an appropriate combining technique, the channel fading effects could be reduced and the sensing performance is thus improved. In this paper, two combining methods are considered. First the Maximum Ratio Combining (MRC) method is presented since it maximizes the sensing performance [19] and the SNR at the output of the combiner, ρ_{output} [20]:

$$\rho_{output} = \sum_{i=1}^{M} \rho_i \tag{2}$$

where ρ_i is the SNR on branch i.

However, this optimal combining method requires the knowledge of the CSI from primary base station at the secondary terminal. Since in a realistic CR scenario the secondary user is not aware of the CSI from the primary base station, this method is only given as an optimal combining method for the sake of comparison with a second method, the Square Law Combining (SLC) method, where the knowledge of CSI from the primary base station is not required.

A modified energy detector is considered in order to differentiate the two hypothesis H_0 and H_1. With this detector the decision is based on the normalized quantity E=$2E_r/N_0$ where E_r is the Band-Pass(BP) representation of the energy of the signal denoted $y(t)$ at the combiner output and N_0 is the one-sided noise PSD

$$E = \frac{2}{N_0}\int_0^T y^2(t)dt = \frac{1}{N_0 W}\sum_{i=1}^{N} {y_i}^2 \tag{3}$$

where y_i denotes the samples obtained by sampling y(t) at the Nyquist frequency $2W$ and N= 2TW is the total number of samples.

A signal will be considered as detected in the bandwidth W and during the observation time T, if the resulting modified energy at the combiner output is higher than a fixed threshold. Considering a detection threshold, η, the probability of detection, P_d, and the probability of false alarm, P_{FA}, are defined by :

$$P_d = P[E > \eta | H_1] \tag{4}$$

$$P_{FA} = P[E > \eta | H_0] \tag{5}$$

In the following analysis, the case of a deterministic channel h_i between the primary transmitter and the i^{th} CR receiver is first investigated. Then, the case of a Rayleigh fading channel is studied where two diversity cases will be considered: Multipolar and Multi-antenna unipolar cases. In the multi-antenna unipolar reception scenario, all the sub channels experience the same Rayleigh fading process with the same Rayleigh distribution parameter σ_h:

$$|h_i| \sim Rayleigh(\sigma_h) \tag{6}$$

On the other hand, in the multi-polar reception scenario, each subchannel h_i experiences a different Rayleigh fading process with a different Rayleigh distribution parameter σ_{hi},

$$|h_i| \sim Rayleigh(\sigma_{hi}) \tag{7}$$

due to the cross-polar discriminations (XPD) which exists between the three polarizations. The XPD denotes the amount of leakage from one polarization to another caused by the channel. This leads to different path-loss pattern for each polarization. A measurement campaign was realized in an outdoor-to-indoor scenario in order to characterize the path-loss as a fonction of distance for each of the three receive polarizations. This measurement campaign is described later in this paper.

In the following, analytical expressions of P_d and P_{FA} are given for MRC and SLC techniques and in a general case where each subchannel experiences a different Rayleigh fading process. In this context, this analytical development has already been made in [14] for the SLC technique but is new for the MRC technique which is given only for the sake of comparison as an optimal combining method. Then, the application of the analytical expressions in a real-world scenario is given, based on a measurement campaign.

3. Deterministic channel

Let's first consider a deterministic channel h_i between the PTx and each of the CR antennas.

3.1. MRC

Under the null hypothesis H_0 the combined signal $y(t)$ at the combiner output is given by:

$$y(t) = \sum_{i=1}^{M} h_i^* n_i(t) \tag{8}$$

where h_i^* is the complex conjugate of the channel h_i

Equation (3) gives:

$$E = \frac{1}{N_0 W} \sum_{k=1}^{N} y_k^2 = \frac{1}{N_0 W} \sum_{k=1}^{N} \left(\sum_{i=1}^{M} h_i^* n_{ik} \right)^2 \tag{9}$$

This can be rewritten as:

$$E = \alpha_h^2 \frac{\sum_{k=1}^{N} \left(\sum_{i=1}^{M} h_i^* n_{ik} \right)^2}{N_0 W {\alpha_h}^2} = \alpha_h^2 E' \tag{10}$$

where $\alpha_h^2 = \sum_{i=1}^{M} |h_i|^2$.

Considering iid n_{ik} with distribution $N(0, N_0W)$ $+ jN(0, N_0W)$, the variable $\sum_{i=1}^{m} h_i^* n_{ik} \sim N(0, N_0W$ $\alpha_h^2) + jN(0, N_0W\alpha_h^2)$. As a result, E' follows a Chi-square distribution with $2N$ degrees of freedom (χ_{2N}^2) .The cumulative distribution function (cdf) of E is then given by :

$$cdf_E(y) = cdf_{E'}(\frac{y}{\alpha_h^2}) = \frac{\gamma(N, y/2\alpha_h^2)}{\Gamma(N)} \tag{11}$$

where $\gamma(..,..)$ is the lower incomplete gamma function and $\Gamma(..)$ denotes the Gamma function [21].

The probability of false-alarm is then given by:

$$\begin{aligned} P_{FA} &= P[E > \eta | H_0] = 1 - P[E < \eta | H_0] \\ &= 1 - cdf_E(\eta) = 1 - \frac{\gamma(N, \eta/2\alpha_h^2)}{\Gamma(N)} \\ &= \frac{\Gamma(N) - \gamma(N, \eta/2\alpha_h^2)}{\Gamma(N)} = \frac{\Gamma(N, \eta/2\alpha_h^2)}{\Gamma(N)} \end{aligned} \tag{12}$$

where $\Gamma(..,..)$ is the upper incomplete gamma function [21].

Under the hypothesis H_1 :

$$y(t) = \sum_{i=1}^{M} h_i^* r_i(t) = \sum_{i=1}^{M} h_i^* (h_i s(t) + n(t)) \tag{13}$$

$$E = \frac{1}{N_0 W} \sum_{k=1}^{N} y_k^2 = \frac{1}{N_0 W} \sum_{k=1}^{N} \left(\sum_{i=1}^{M} |h_i|^2 s_k + h_i^* n_{ik} \right)^2 \tag{14}$$

This can be rewritten as:

$$E = \alpha_h^2 \frac{\sum_{k=1}^{N} \left(\sum_{i=1}^{M} |h_i|^2 s_k + h_i^* n_{ik} \right)^2}{\alpha_h^2 N_0 W} = \alpha_h^2 E'' \tag{15}$$

Considering iid n_{ik} with distribution $N(0, N_0W)+$ $jN(0, N_0W)$, E" follows a non central chi square distribution with 2N degrees of freedom and the non centrality parameter $\lambda = 2\sum_{i=1}^{M} \rho_i = 2\rho_{output}$ ($E'' \sim \chi_{2N}^2(2\rho_{output})$

The probability of detection is then obtained by :

$$\begin{aligned} P_d = P(E > \eta | H_1) &= P(\alpha_h^2 E'' > \eta | H_1) \\ &= P(E'' > \frac{\eta}{\alpha_h^2} | H_1) \end{aligned} \tag{16}$$

Using [22], we can obtain the following closed-form expression:

$$P_d = Q_N(\sqrt{2\rho_{output}}, \sqrt{\frac{\eta}{\alpha_h^2}}) \tag{17}$$

where $Q_N(.,.)$ is the generalized Marcum Q function [23].

3.2. SLC

Using the SLC method, the combined signal $y(t)$ at the combiner output is given by:

$$y(t) = \sqrt{\sum_{i=1}^{M} r_i^2(t)} \tag{18}$$

Using the same approach than the one used above in the MRC case, as has been done in [14], the analytical expressions of P_d and P_{FA} for the

SLC method and in a deterministic channel scenario are given by :

$$P_{FA} = \frac{\Gamma(NM, \eta/2)}{\Gamma(NM)} \tag{19}$$

$$P_d = Q_{NM}(\sqrt{2\rho_{output}}, \sqrt{\eta}) \tag{20}$$

4. Rayleigh fading channel

The mean probability of detection $\overline{P_d}$ for correlated Rayleigh fading channels is obtained by averaging the probability of detection for deterministic channels (20) and (17) over the pdf of ρ_{output} referred to as $f(\rho_{output})$:

$$\overline{P_d} = \int_0^\infty P_d(\rho_{output}) f(\rho_{output}) d\rho_{output} \tag{21}$$

It is shown in Appendixe 1, how we obtain the analytical expressions of the pdf of ρ_{output} for correlated channels and in a multi-polar reception scenario. The final result of this development is given in the following.

The pdf of ρ_{output} for correlated Rayleigh fading channels is given by:

$$f(\rho) = \frac{1}{\gamma}[\frac{e^{Z_1\rho}}{(Z_1 - Z_2)(Z_1 - Z_3)} + \frac{e^{Z_2\rho}}{(Z_2 - Z_3)(Z_2 - Z_1)} + \frac{e^{Z_3\rho}}{(Z_3 - Z_1)(Z_3 - Z_2)}] \tag{22}$$

where ρ_{ij} is the complex correlation coefficient between the i^{th} and j^{th} antenna. and Z_1, Z_2 and Z_3 are the poles of $\frac{1}{(Z^3 + \frac{\beta}{\gamma}Z^2 + \frac{\alpha}{\gamma}Z + \frac{1}{\gamma})}$ and :

$$\alpha = \overline{\rho_1} + \overline{\rho_2} + \overline{\rho_3}$$

$$\beta = \overline{\rho_1\rho_2} - |\rho_{12}|^2 \overline{\rho_1\rho_2} + \overline{\rho_1\rho_3} - |\rho_{13}|^2 \overline{\rho_1\rho_3} + \overline{\rho_2\rho_3} - |\rho_{23}|^2 \overline{\rho_2\rho_3}$$

$$\gamma = \overline{\rho_1\rho_2\rho_3} - |\rho_{12}|^2 \overline{\rho_1\rho_2\rho_3} - |\rho_{13}|^2 \overline{\rho_1\rho_2\rho_3} - |\rho_{23}|^2 \overline{\rho_1\rho_2\rho_3} + \rho_{12}\rho_{23}\rho_{13}^* \overline{\rho_1\rho_2\rho_3} + \rho_{13}\rho_{12}^*\rho_{23}^* \overline{\rho_1\rho_2\rho_3}$$

where $\overline{\rho_i}$ is the mean SNR received on the i^{th} antenna.

5. Experimental setup

A measurement campaign has been realized in order to simulate the theoretical results obtained in the previous sections. The principal aim of these measurements was to obtain in a practical case, the mean received power and SNR of the three polarizations at the receive antennas, for different distances between the primary transmitter and the secondary terminal.

5.1. Measurement scenario

An Outdoor-to-Indoor scenario was considered where an indoor cognitive radio terminal senses the signals from an outdoor primary transmitter. The measurement site was the third floor of Building U at Solbosch campus of Brussels University. The transmitter was fixed on the rooftop of a neighboring building (Building L), at a total height of 15 m and was directed toward the measurement site (Figure. 1). A brick wall blocked the LOS direction. The measurements were performed in a total of 78 positions, located in seven successive rooms. The rooms were separated by brick walls and closed wooden doors. The distance between the transmitter and the measurement points was in the range of 30 to 80 meters.

In order to obtain the mean power values of each of the three received polarizations, at each measurement position, a total of 64 spatially separated measurements were taken in an 8×8 grid. The spacing between grid points was $\lambda/2$ (4 cm). At each grid point, 5 snapshots of the received signal were sampled and averaged to increase the SNR.

5.2. Measurement equipment

The measurement was performed using a Vector Signal Generator (Rohde & Schwarz SMATE200A VSG) at the transmitter side and a Signal Analyzer (Rohde & Schwarz FSG SA) at the receiver side. The Tx chain was composed of the VSG and a unipolar directional antenna with one vertical and one horizontal polarization. The Rx antenna was a tri-polarized antenna, made of three co-located perpendicular omnidirectional antennas. The three receive antennas were fixed on an automatic positioner to create a virtual planar array,

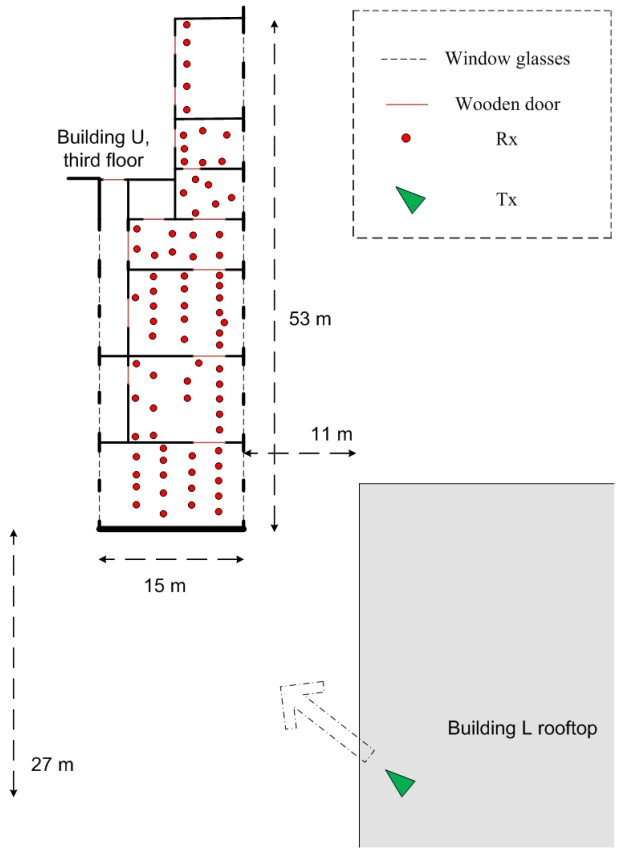

Figure 1: Measurement setup

and were selected one after another by means of a switch. They were connected to the Signal Analyzer through a 25 dB low-noise amplifier. A CW signal at the frequency of 3.5 GHz was transmitted and the corresponding frequency response was recorded at the receiver side. The antenna input power was 19 dBm.

6. Results

By fitting the mean power values of the sub-channels obtained by averaging the 64 received power values in the 8×8 grid, a path-loss model was established for each of these sub-channels. An exemple of a path-loss model obtained from the measurements is given in figure. 2. An overview of the different path-loss equations is given in Table. 1. The theoretical expressions found in the previous sections are simulated using these path-loss models. The simulations were made using a pre-specified probability of false alarm $P_{FA} = 0.01$ and a fixed value of the time bandwidth product TW=5 (N=10). The noise variance N_0W was fixed to -70dBm.

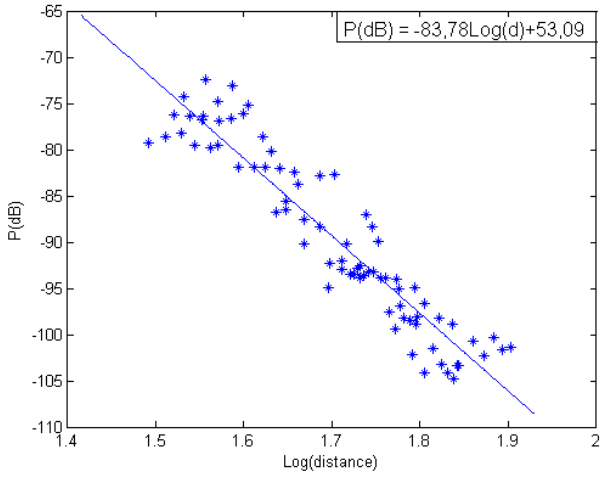

Figure 2: Path loss fitting for TX_H - RX_V

Table 1: Path-loss equations[1]

$TX_V\ RX_V$	$P(dB) = -76.51Log\,(D(m)) + 44.59$
$TX_V\ RX_{H1}$	$P(dB) = -71.89Log\,(D(m)) + 32.05$
$TX_V\ RX_{H2}$	$P(dB) = -66.29Log\,(D(m)) + 22.87$
$TX_H\ RX_V$	$P(dB) = -83.78Log\,(D(m)) + 53.09$
$TX_H\ RX_{H1}$	$P(dB) = -87.97Log\,(D(m)) + 65.35$
$TX_H\ RX_{H2}$	$P(dB) = -77.40Log\,(D(m)) + 46.12$

6.1. *Polarization and space diversity for uncorrelated channels*

The probability of detection versus both the distance between the PTx and the STE, and the SNR at the receive horizontal antenna (RX_{H1}) is shown for different diversity cases in figure. 3. The sensing performance of the single-antenna case, the polarization diversity case and the space diversity case (M=3) are compared with each other. The probability of detection is obtained by numerically integrating (21) for different distances.

[1] $TX_H\ RX_V$ denotes the link between the horizontally polarized antenna at the transmitter and the vertically polarized antenna at the receiver. RX_{H1} and RX_{H2} stand for the two horizontally polarized antenna at the receiver. P denotes the received power in dB scale. D denotes the distance in meter between the transmitter and the receiver

The threshold η is numerically obtained for each distance to meet the false-alarm probability constraint.

As shown in this figure, in a single antenna case, the orientation of the secondary CR antenna has a significant negative impact on the detection performance when it differs with the orientation of the primary transmitter antenna. In a practical case where the orientation of the STE does not stay the same all the time, the sensing performance could then be significantly deteriorated. As shown in this figure, the use of diversity considerably improves the sensing performance. By considering a minimum acceptable detection probability of 0.95, the use of diversity increases the range of acceptable sensing up to 18 meters. The minimum acceptable SNR is reduced up to 14 dB.

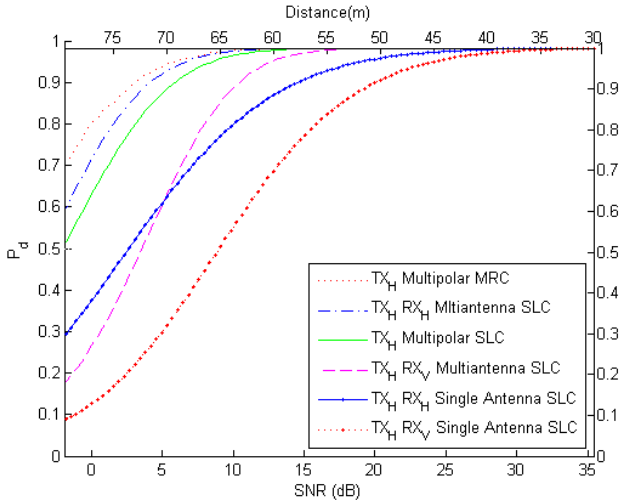

Figure 3: Multi-antenna Multi-polar and single antenna comparison for TX_H and M=3

As expected, the best performances are obtained by the MRC method. However this optimal method requires the knowledge of the primary to secondary CSI which is not practical in a realistic CR scenario. The detection performances are slightly decreased by using the SLC method where the knowledge of the primary to secondary CSI is not anymore required. For exemple for the multi-polar reception scenario, the SLC method increases the minimum acceptable SNR by less than 2 dB and decreases the range of acceptable sensing by less than 3 meters.

For the same combining method, the best performance is obtained when using three separated receive antennas with the same orientation as the orientation of the PTx. The performance of the tri-polarized sensing lies between the spatial diversity cases with co and cross-orientation between PTx and STE. At lower SNR and in case of cross orientation between the PTx and the STE, the sensing performance of a CR system using spatial diversity could even become worse than a single antenna system having the same orientation than the PTx. In a practical case, where the orientation of the secondary terminal does not stay the same all the time, the use of a tri-polarized antenna scheme at the secondary terminal is a good trade-off of performance.

Also as shown in figure. 4, in a practical case where the orientation of the PTx is unknown, the use of a tri-polarized antenna scheme at the secondary terminal is a good trade-off of performance compared to the spatial diversity case, since all the receive polarizations are taken into account. In addition, by using the multi-polarized sensing, we can considerably improve the sensing performance while having a compact antenna system.

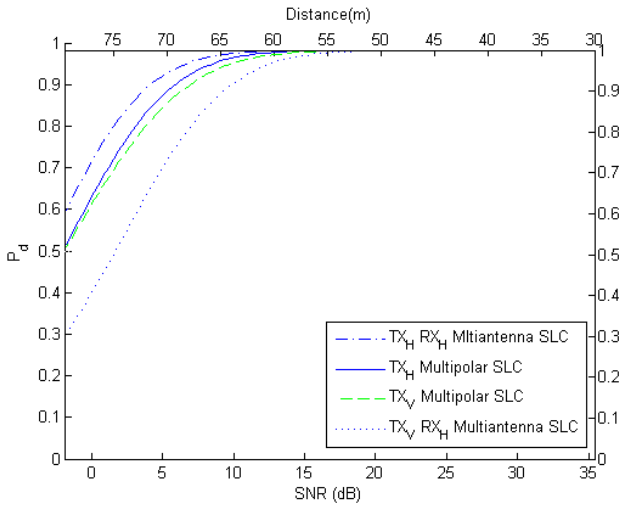

Figure 4: Multi-antenna and Multi-polar performance when the TX orientation is unknown (M=3)

6.2. Inter-antenna correlation effect on P_d

For the multi-polarized sensing case, based on the results obtained in [24], a normal distribution with mean 0.36 and standard deviation of 0.19 is

considered for the amplitude of the inter-antenna correlation. Based on the same paper, the phase of the inter-antenna correlation parameters is considered to be uniformly distributed. Figure. 5 shows that, as expected, by increasing the amplitude of correlation between the antennas, the sensing performances are deteriorated but even with a high inter-antenna correlation, the performances of tri-polarized sensing remains considerably better than single antenna sensing.

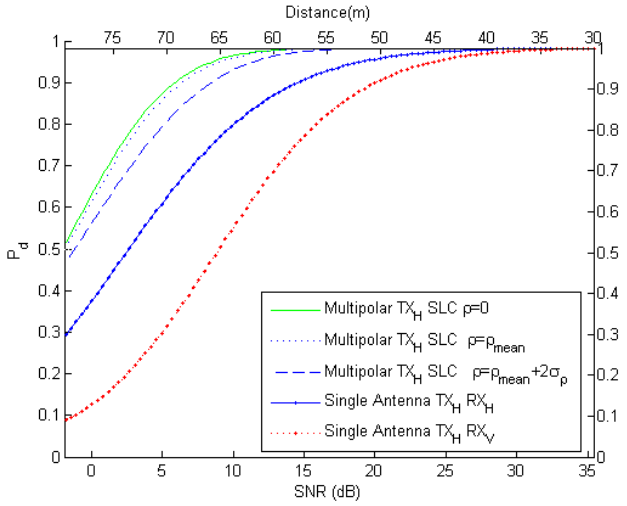

Figure 5: Inter-antenna correlation effect on the tri-polarized sensing and comparison with the single antenna case

7. Conclusion

In this paper the performance of multi-polarized spectrum sensing based on energy detection was studied and compared to a multi-antenna co-polar system. A theoretical formulation was made and applied to a real-world scenario, based on an outdoor to indoor measurement campaign. The detection probability versus the distance between the PTx and the STE was analyzed for the different cases. It was shown that the poor sensing performance of a single antenna system could be significantly improved by the use of polarization and spatial diversity. It has been found that in a multi-paths environment, the performance of spectrum sensing by spatial diversity could be deteriorated depending on the matching between the orientation of the PTx and the STE. In a practical case where the orientation of the STE is not the same all the time and the orientation of the PTx is not known by the secondary user, the spectrum sensing by polarization diversity scheme takes into account all the received polarizations and is thus a good compromise of performance. Moreover while space diversity scheme requires large spacing between antennas, the use of co-located tri-polarized antennas, let the STE to be almost as compact as a single antenna system while having a significant better performance. As expected, the inter-antenna correlation was found to have a negative impact on the sensing performance. However, even with high inter-antenna correlation, the performance of tri-polarized sensing remains considerably better than the single antenna case.

APPENDIX 1

The analytical expressions of the pdf of ρ_{output} for correlated channels and in a multi-polar scenario using MRC and energy detector are derived by using the process used in [25]. The Laplace transform of $f(\rho_{output})$ is first deduced by:

$$F(Z) = \mathscr{L}(f(\rho_{output})) = \int_0^\infty f(\rho_{output}) e^{-Z\rho_{output}} d\rho_{output} = |I + Z\mathbf{L}|^{-1} \quad (23)$$

where I is the identity matrix and:

$$\mathbf{L} = \begin{pmatrix} \overline{\rho_1} & \rho_{12}^* \sqrt{\overline{\rho_1 \rho_2}} & \rho_{13}^* \sqrt{\overline{\rho_1 \rho_3}} \\ \rho_{12} \sqrt{\overline{\rho_1 \rho_2}} & \overline{\rho_2} & \rho_{23}^* \sqrt{\overline{\rho_2 \rho_3}} \\ \rho_{13} \sqrt{\overline{\rho_1 \rho_3}} & \rho_{23} \sqrt{\overline{\rho_2 \rho_3}} & \overline{\rho_3} \end{pmatrix} \quad (24)$$

where ρ_{ij} is the complex correlation coefficient between the i^{th} and j^{th} antenna.

The $f(\rho_{output})$ is then obtained by the inverse Laplace transform of F(Z):

$$f(\rho_{output}) = \mathscr{L}^{-1}(F(Z)) = \frac{1}{2\pi j} \oint e^{ZS} F(Z) dZ \quad (25)$$

by developing $|I + Z\mathbf{L}|^{-1}$, the following expression is obtained :

$$|I + Z\mathbf{L}|^{-1} = \frac{1}{1 + \alpha Z + \beta Z^2 + \gamma Z^3} = \frac{1}{\gamma(Z^3 + \frac{\beta}{\gamma}Z^2 + \frac{\alpha}{\gamma}Z + \frac{1}{\gamma})} \quad (26)$$

where :

$$\alpha = \overline{\rho_1} + \overline{\rho_2} + \overline{\rho_3}$$

$$\beta = \overline{\rho_1\rho_2} - |\rho_{12}|^2 \overline{\rho_1\rho_2} + \overline{\rho_1\rho_3} - |\rho_{13}|^2 \overline{\rho_1\rho_3} + \overline{\rho_2\rho_3} - |\rho_{23}|^2 \overline{\rho_2\rho_3}$$

$$\gamma = \overline{\rho_1\rho_2\rho_3} - |\rho_{12}|^2 \overline{\rho_1\rho_2\rho_3} - |\rho_{13}|^2 \overline{\rho_1\rho_2\rho_3} - |\rho_{23}|^2 \overline{\rho_1\rho_2\rho_3} + \rho_{12}\rho_{23}\rho_{13}^*\overline{\rho_1\rho_2\rho_3} + \rho_{13}\rho_{12}^*\rho_{23}^*\overline{\rho_1\rho_2\rho_3}$$

Let Z_1,Z_2 and Z_3 be the three poles of $\frac{1}{(Z^3 + \frac{\beta}{\gamma}Z^2 + \frac{\alpha}{\gamma}Z + \frac{1}{\gamma})}$:

$$F(Z) = |I + Z\mathbf{L}|^{-1} = \frac{1}{\gamma(Z^3 + \frac{\beta}{\gamma}Z^2 + \frac{\alpha}{\gamma}Z + \frac{1}{\gamma})} = \frac{1}{\gamma(Z - Z_1)(Z - Z_2)(Z - Z_3)} \quad (27)$$

The inverse Laplace transform of F(Z) is then obtained by :

$$f(\rho_{output}) = \mathbf{L}^{-1}(F(Z)) = \frac{1}{\gamma}[\frac{e^{Z_1\rho}}{(Z_1 - Z_2)(Z_1 - Z_3)} + \frac{e^{Z_2\rho}}{(Z_2 - Z_3)(Z_2 - Z_1)} + \frac{e^{Z_3\rho}}{(Z_3 - Z_1)(Z_3 - Z_2)}] \quad (28)$$

References

[1] Next generation/dynamic spectrum access/cognitive radio wireless networks: A survey, Computer Networks 50 (13) (2006) 2127 – 2159. doi:DOI: 10.1016/j.comnet.2006.05.001.

[2] FCC, Spectrum policy task force report, ET Docket (02-135).

[3] S. Haykin, Cognitive radio: brain-empowered wireless communications, Selected Areas in Communications, IEEE Journal on 23 (2) (2005) 201 – 220. doi:10.1109/JSAC.2004.839380.

[4] D. Cabric, S. Mishra, D. Willkomm, R. Brodersen, A. Wolisz, A cognitive radio approach for usage of virtual unlicensed spectrum, 2005.

[5] A. Sahai, N. Hoven, R. Tandra, Some fundamental limits in cognitive radio, 2004.

[6] D. Cabric, S. Mishra, R. Brodersen, Implementation issues in spectrum sensing for cognitive radios, in: Signals, Systems and Computers, 2004. Conference Record of the Thirty-Eighth Asilomar Conference on, Vol. 1, 2004, pp. 772 – 776 Vol.1. doi:10.1109/ACSSC.2004.1399240.

[7] H. Urkowitz, Energy detection of unknown deterministic signals, Proceedings of the IEEE 55 (4) (1967) 523 – 531.

[8] D. Cabric, A. Tkachenko, R. W. Brodersen, Experimental study of spectrum sensing based on energy detection and network cooperation, in: TAPAS '06: Proceedings of the first international workshop on Technology and policy for accessing spectrum, ACM, New York, NY, USA, 2006, p. 12. doi:http://doi.acm.org/10.1145/1234388.1234400.

[9] A. Al-Abbasi, T. Fujii, A novel spectrum sensing method using multi-antennas without channel state information, in: Wireless Communication Systems, 2009. ISWCS 2009. 6th International Symposium on, 2009, pp. 373 –377. doi:10.1109/ISWCS.2009.5285330.

[10] V. Kuppusamy, R. Mahapatra, Primary user detection in ofdm based mimo cognitive radio, in: Cognitive Radio Oriented Wireless Networks and Communications, 2008. CrownCom 2008. 3rd International Conference on, 2008, pp. 1 –5. doi:10.1109/CROWNCOM.2008.4562561.

[11] S. Kim, J. Lee, H. Wang, D. Hong, Sensing performance of energy detector with correlated multiple antennas, Signal Processing Letters, IEEE 16 (8) (2009) 671 –674. doi:10.1109/LSP.2009.2021381.

[12] R. Mahapatra, Wideband spectrum sensing in multiantenna based cognitive radio, in: India Conference (INDICON), 2009 Annual IEEE, 2009, pp. 1 –3. doi:10.1109/INDCON.2009.5409461.

[13] W. Ma, M. Q. Wu, D. Liu, M. L. Wang, User sensing based on mimo cognitive radio sensor networks, in: Computer Science and Information Technology, 2009. ICCSIT 2009. 2nd IEEE International Conference on, 2009, pp. 205 –208. doi:10.1109/ICCSIT.2009.5234387.

[14] F. F. Digham, M.-S. Alouini, M. K. Simon, On the energy detection of unknown signals over fading channels, Communications, IEEE Transactions on 55 (1) (2007) 21 –24. doi:10.1109/TCOMM.2006.887483.

[15] A. Pandharipande, J.-P. Linnartz, Performance analysis of primary user detection in a multiple antenna cognitive radio, in: Communications, 2007. ICC '07. IEEE International Conference on, 2007, pp. 6482 – 6486. doi:10.1109/ICC.2007.1072.

[16] B. Lindmark, M. Nilsson, On the available diversity gain from different dual-polarized antennas, Selected Areas in Communications, IEEE Journal on 19 (2) (2001) 287 –294. doi:10.1109/49.914506.

[17] P. Kyritsi, D. Cox, R. Valenzuela, P. Wolniansky, Effect of antenna polarization on the capacity of a multiple element system in an indoor environment, Selected Areas in Communications, IEEE Journal on 20 (6) (2002) 1227 – 1239. doi:10.1109/JSAC.2002.801225.

[18] L. Lukama, K. Konstantinou, D. Edwards, Performance of a three-branch orthogonal polarization diversity scheme, in: Vehicular Technology Conference, 2001. VTC 2001 Fall. IEEE VTS 54th, Vol. 4, 2001, pp. 2033 –2037 vol.4. doi:10.1109/VTC.2001.957101.

[19] J. Ma, Y. Li, Soft combination and detection for cooperative spectrum sensing in cognitive radio networks, 2007, pp. 3139 –3143. doi:10.1109/GLOCOM.2007.594.

[20] A. Goldsmith, Wireless Communications, Cambridge University Press, New York, NY, USA, 2005.

[21] I. R. I.S. Gradshteyn, Table of Integrals, Series and products, 6th ed., San Diego, CA Academic, 2000.

[22] J. Marcum, A statistical theory of target detection by pulsed radar, Information Theory, IRE Transactions on (2) 59–267. doi:10.1109/TIT.1960.1057560.

[23] A. Nuttall, Some integrals involving the Q_M function, IEEE Transactions on Information Theory.

[24] F. Quitin, F. Bellens, A. Panahandeh, J.-M. Dricot, F. Dossin, C. Oestges, F. Horlin, P. D. Doncker, A time-variant statistical channel model for tripolarized antenna systems, in: PIMRC 2010, Istanbul Turkey, 2010.

[25] J. Pierce, S. Stein, Multiple diversity with nonindependent fading, Proceedings of the IRE 48 (1) (1960) 89 –104. doi:10.1109/JRPROC.1960.287384.